PHYSICAL REVIEW B **94**, 020411(R) (2016)

Domain wall in a quantum anomalous Hall insulator as a magnetoelectric piston

Pramey Upadhyaya and Yaroslav Tserkovnyak
Department of Physics and Astronomy, University of California, Los Angeles, California 90095, USA
(Received 30 December 2015; revised manuscript received 22 June 2016; published 25 July 2016)

We theoretically study the magnetoelectric coupling in a quantum anomalous Hall insulator state induced by interfacing a dynamic magnetization texture to a topological insulator. In particular, we propose that the quantum anomalous Hall insulator with a magnetic configuration of a domain wall, when contacted by electrical reservoirs, acts as a magnetoelectric piston. A moving domain wall pumps charge current between electrical leads in a closed circuit, while applying an electrical bias induces reciprocal domain-wall motion. This pistonlike action is enabled by a finite reflection of charge carriers via chiral modes imprinted by the domain wall. Moreover, we find that, when compared with the recently discovered spin-orbit torque-induced domain-wall motion in heavy metals, the reflection coefficient plays the role of an effective spin-Hall angle governing the efficiency of the proposed electrical control of domain walls. Quantitatively, this effective spin-Hall angle is found to approach a universal value of 2, providing an efficient scheme to reconfigure the domain-wall chiral interconnects for possible memory and logic applications.

DOI: 10.1103/PhysRevB.94.020411

Introduction. Motivated by the possibility of realizing unique magnetoelectric phenomena, the breaking of time-reversal symmetry in recently discovered topological insulators (TIs) [1] has become one of the central themes of theoretical and experimental research. In particular, a proximal magnetic order can induce a gap in an otherwise linear spectrum of Dirac electrons residing on the surface of a TI, resulting in a phase transition to a quantum anomalous Hall (QAH) state [2]. This QAH phase manifests itself via the appearance of quantized surface Hall currents and chiral modes (at the boundary where the gap vanishes), which, in turn, give rise to two types of magnetoelectric effects. First, the Oersted fields originating from the surface Hall currents result in a topological magnetoelectric effect [3] (a condensed matter realization of axion electrodynamics [4]). Examples of predicted consequences of this magnetoelectric effect include the appearance of image magnetic monopole [5] and charging of magnetization textures [6]. Second, the surface Hall currents and chiral modes exert exchange coupling-induced spin torque on the magnetic order both in and out of equilibrium. Here, the magnetoelectric effects explored theoretically include surface Hall current-induced switching of monodomain magnets [7], coupled dynamics of the domain wall and chiral mode imprinted by the wall [8,9], and equilibrium spin torque-induced interfacial anisotropy and Dzyaloshinskii-Moriya interaction [10].

Technologically, the magnetoelectric effects in the QAH regime provide an opportunity to construct spintronic devices with minimal dissipation [7], owing to the dissipationless nature of Hall currents and chiral propagation. A prototypical example of a spintronic application envisioned for next generation information processing is based on a domain wall, owing to its nonvolatile nature. In such a device, information stored in a domain-wall configuration is manipulated electrically [11] for memory (such as racetrack memory [12]) and logic [13] applications. However, mitigating Joule heating incurred during this electrical manipulation is one of the major challenges [12], demanding the search for alternate mechanisms to control domain configurations electrically. A natural question then arises as to the possibility of taking advantage of low-dissipation magnetoelectric effects in the QAH phase for this purpose. In this Rapid Communication, we answer this question affirmatively by proposing an energy-efficient scheme to move domain walls electrically, exploiting the magnetoelectric coupling mediated by the chiral modes in the QAH regime. On another front, magnetic-field-induced domain dynamics has recently been visualized in the QAH phase [14], resulting in dissipation [15] and fragility of the perfect quantization [16]. To this end, the proposed current-induced domain dynamics adds an experimental knob to explore nonequilibrium phenomena in the QAH regime.

Main results. The proposed system consists of a single domain wall, separating domains with spins oriented perpendicular (i.e., along $\pm z$) to the plane of the TI film (see Fig. 1). This system is motivated by a recent experimental observation of the QAH effect in a magnetically doped TI [17] and giant spin-orbit torque-induced switching of perpendicular magnets [18] in the same system. The opposite out-of-plane magnetizations, in the respective domains, open gaps of opposite signs. This results in "local" QAH states with chiral edge modes propagating in opposite directions on the same edge of the sample (shown by the red and green lines, respectively). At the domain wall, the out-of-plane component, and hence the gap, vanishes, imprinting two comoving chiral modes [1]. The magnetoelectric system is then formed by connecting the film to two electrical leads, as shown in Fig. 1.

We begin by summarizing the two main results of this Rapid Communication, i.e., Eqs. (1) and (2), which will be derived later. First, the motion of the domain wall pumps charge current between the reservoirs maintained at the same electrochemical potential. For a domain wall moving with a velocity v in a mirror- (about the xz plane) symmetric system, this pumped current is given by

$$I_p = evk_F R/\pi. \tag{1}$$

Here, e is the charge of an electron, k_F is the Fermi wave number of electrons propagating along the chiral modes, and R is the reflection coefficient of the domain-wall region (from the view of the edge modes). This phenomenon is found to

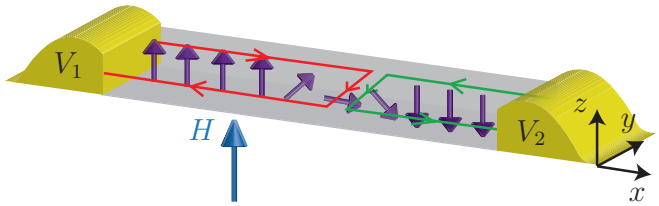

FIG. 1. Schematic of the magnetoelectric system: A magnetically doped topological insulator with the configuration of a domain wall connected by two electrical leads that can be maintained at voltages V_1 and V_2. The domain-wall configuration results in opposite quantum anomalous Hall effects in two domains, with the presence of chiral edge modes as indicated by the red and green lines. An external magnetic field can be applied to move the domain wall.

be similar to the particle current dragged by a piston, having a reflectivity R, moving through a gas of particles. Second, sending current through the chiral modes (for example, by application of an external voltage V between the reservoirs) induces motion of the domain wall. The corresponding domain-wall velocity is given by $v = \gamma H_V \delta_w/\alpha$, with γ, δ_w, and α being the gyromagnetic ratio, domain-wall width, and Gilbert damping, respectively. Here, we have defined an electrical bias-induced effective magnetic field as

$$H_V = \frac{\pi\theta_V \hbar I_q}{2e\lambda_F M_s d W}, \tag{2}$$

with $I_q \equiv e^2 V/h$ being the Landauer-Büttiker current through a single mode and $\theta_V \equiv 4R$. Here, $\hbar$ is the reduced Planck's constant, $\lambda_F \equiv 2\pi/k_F$ is the Fermi wavelength, while M_s, d, and W are the saturation magnetization, thickness, and the width of the magnetically doped TI film, respectively. Recently, utilizing spin-orbit interaction has emerged as an efficient scheme for moving domain walls. In one popular scheme, the ferromagnet is interfaced with a heavy metal which, via a spin-Hall-like mechanism, applies torque to induce domain-wall motion [19]. The effective drive field for such a mechanism is given by $H_S = \pi\theta_S \hbar I/2et_m M_s d W$, where t_m is the thickness of the heavy metal and the efficiency of the drive field is given by the so-called spin-Hall angle θ_S (more precisely, referred to as the spin-Hall tangent [20]). Comparing H_V with H_S, we note that θ_V plays the role of efficiency, much as the spin-Hall angle. Moreover, we show that with increasing sample width, when the reflection coefficient approaches 0.5, the effective spin-Hall efficiency reaches a universal value of $\theta_V = 2$, for the proposed mechanism. For typical heavy metals, $\theta_S \sim 0.1$ [21], suggesting the QAH regime could be an attractive alternative for efficient electrical manipulation of domains. Furthermore, dissipation in the QAH regime is localized only at the domain wall and the electrical contacts. Consequently, the QAH phase has the advantage of dissipation scaling with the number of domain walls, as opposed to the entire length of the magnetic sample outside of the QAH regime [12].

Model. The magnetic sector, exchange coupled to Dirac electrons on the surface of TI, is described by the free energy [8]

$$\mathcal{F}_M = \int d^3r \left(\frac{A|\nabla \mathbf{m}|^2}{2} + \frac{K m_z^2}{2} + D m_z \nabla \cdot \mathbf{m} - H M_s m_z \right), \tag{3}$$

where $\mathbf{m} \equiv (m_x, m_y, m_z)$ is a unit vector oriented along the magnetization, H is a z-directed external magnetic field, and we have defined $\nabla \equiv \mathbf{x}\partial_x + \mathbf{y}\partial_y$. Phenomenologically, the parameters A and K represent the strength of the exchange interaction and perpendicular anisotropy in the magnet, respectively, while D parametrizes any inversion symmetry-breaking-induced interfacial Dzyaloshinskii-Moriya interaction [22] (for example, due to different materials on the top and bottom of the magnetic TI film). We focus on the configuration of a one-dimensional domain wall and adopt the collective coordinate approach [23] to describe its dynamics. To this end, the free energy $\mathcal{F}_M$ can be expressed in terms of X and Φ by substitution of a Walker wall ansatz [24] $\ln\{\tan[\theta(x)/2]\} = (x - X)/\delta_w$, $\phi(x) = \Phi$ in Eq. (3). Here, we have parametrized the magnetization field in terms of the polar and azimuthal angles as $\mathbf{m} \equiv (\sin\theta\cos\phi, \sin\theta\sin\phi, \cos\theta)$, while X and Φ label, respectively, the position and the azimuthal angle of the domain-wall magnetization at the location where its out-of-plane component vanishes. Adding the electrical reservoirs, we then arrive at the free energy for our magnetoelectric system as

$$\mathcal{F}(Q, X, \Phi) = -2M_s d W (HX + H_D \delta_w \cos\Phi) - QV. \tag{4}$$

Here, we have defined an effective Dzyaloshinskii-Moriya field $H_D \equiv \pi D/2M_s\delta_w$. The electronic degrees of freedom of the reservoirs are represented by a single thermodynamic variable $Q \equiv (Q_1 - Q_2)/2$, with Q_1 and Q_2 denoting the electrical charge in reservoirs 1 and 2, respectively. The conjugate force, $V \equiv V_1 - V_2$, is the voltage difference between the respective contacts. Such a reduction to a single variable Q can be done assuming $\dot{Q}_1 + \dot{Q}_2 = 0$ (i.e., no charge is being deposited in the QAH region), whose applicability will be discussed later.

Within the linear response, the out-of-equilibrium dynamics is then governed by [25]

$$\begin{pmatrix} \dot{Q} \\ \dot{X} \\ \dot{\Phi} \end{pmatrix} = \begin{pmatrix} \mathcal{L}_{qq} & \mathcal{L}_{qx} & \mathcal{L}_{q\phi} \\ \mathcal{L}_{xq} & \mathcal{L}_{xx} & \mathcal{L}_{x\phi} \\ \mathcal{L}_{\Phi q} & \mathcal{L}_{\phi x} & \mathcal{L}_{\phi\phi} \end{pmatrix} \begin{pmatrix} f_Q \\ f_X \\ f_\Phi \end{pmatrix}, \tag{5}$$

where the thermodynamically conjugate forces, identified from Eq. (4), are $f_Q = V$, $f_X = 2M_s t W H$, and $f_\Phi = -2M_s t W H_D \delta_w \sin\Phi$. The kinetic coefficients for the electric and magnetic sector are fixed by the Ohm's law and the substitution of the Walker ansatz into the Landau-Lifshitz-Gilbert equation [26], respectively, as $\mathcal{L}_{qq} = G$, $\mathcal{L}_{xx} = (\gamma/2M_s t W)\alpha\delta_w/(1+\alpha^2)$, $\mathcal{L}_{\phi\phi} = (\gamma/2M_s t W)\alpha/\delta_w(1+\alpha^2)$, and $\mathcal{L}_{\phi x} = -\mathcal{L}_{x\phi} = (\gamma/2M_s t W)/(1+\alpha^2)$. Finally, the proposed magnetoelectric coupling is encoded in $\mathcal{L}_{qx}, \mathcal{L}_{q\phi}$, describing domain-wall dynamics-induced charge pumping, and $\mathcal{L}_{xq}, \mathcal{L}_{\phi q}$, describing the electrical bias-induced domain-wall motion. We next use Büttiker-Brouwer's formalism [27] for deriving the functional form of $\mathcal{L}_{qx}$, followed by the use of

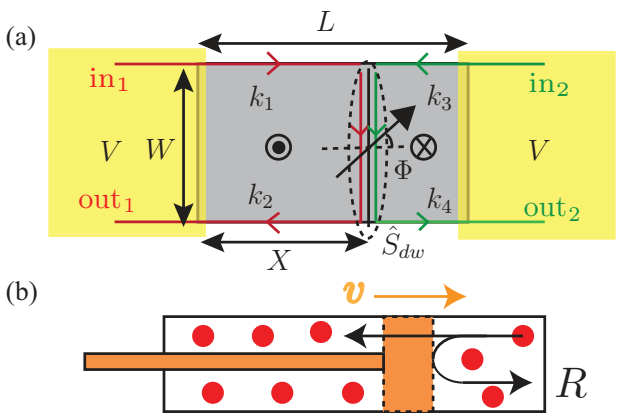

FIG. 2. Schematic depicting the scattering process. (a) Top view of the QAH system of width W and length L, with a domain wall at a distance X from the left contact. The magnetization at the domain-wall center is depicted by the arrow making an angle ϕ with the x axis. Electrical transport occurs via chiral modes at the edges of the sample (with their respective wave vectors denoted by k_i), which, upon reaching the domain-wall region (marked by the dashed ellipse), can intermix. This intermixing is parametrized by a scattering matrix of the wall region $\hat{S}_{dw}$. (b) Schematic of "1D piston" with the gas of particles (represented by the solid circles) constrained to move along the length of the wire. The piston, having an opacity R, is moving with a velocity v through the gas of the particles and can thus drag a flux. This phenomenon, as discussed in the text, is equivalent to the current pumped by the moving domain wall in (a).

Onsager reciprocity, as in Ref. [28], to obtain $\mathcal{L}_{xq}$ and hence the main results of this Rapid Communication.

Charge transport and pumping. The charge pumping by a dynamic domain wall is an example of a parametric pump. The electrical transport between the reservoirs occurs via the chiral modes, as sketched in Fig. 2(a). The modes emanating from the respective contacts reach the domain-wall region without scattering where, via a finite probability to intermix, they can either transmit or reflect. The scattering, in turn, depends parametrically on the location of the domain wall via the propagation phases acquired during the journey of the chiral modes between the reservoirs and the domain wall. Thus, a domain wall moving with a constant velocity, according to the Büttiker-Brouwer's formalism [27], results in the pumping of a charge current. We start by writing down the scattering matrix $\hat{S}$ for the QAH insulator with a domain wall located at a distance X from the left contact. Adopting the following definition for the scattering matrix, $\binom{\text{out}_1}{\text{out}_2} \equiv \hat{S}\binom{\text{in}_1}{\text{in}_2}$, where $\text{in}_1(\text{out}_1)$ and $\text{in}_2(\text{out}_2)$ represent the amplitude of incoming (outgoing) modes from left and right contacts, respectively, we have

$$\hat{S} = \begin{pmatrix} re^{i(k_1+k_2)X} & t'e^{ik_3L}e^{i(k_2-k_3)X} \\ te^{ik_4L}e^{i(k_1-k_4)X} & r'e^{i(k_3+k_4)L}e^{-i(k_3+k_4)X} \end{pmatrix}. \quad (6)$$

Here, L is the length of the QAH insulator between the reservoirs, k_i represent the propagation wave vectors in different sections of the chiral modes, and $\hat{S}_{dw} \equiv \begin{pmatrix} r & t' \\ t & r' \end{pmatrix}$ denotes the scattering matrix of the wall region, which can depend on Φ, as depicted in Fig. 2. Using the Büttiker-Brouwer's formula [i.e., formula (5) from Brouwer's paper in Ref. [27]] on Eq. (6), the charge current pumped by a dynamic domain wall is then given by

$$I_1 = \frac{\gamma e H \delta_w}{2\pi\alpha}(R\{k_1+k_3\}+k_2-k_3),$$
$$I_2 = -\frac{\gamma e H \delta_w}{2\pi\alpha}(R\{k_1+k_3\}+k_4-k_1), \quad (7)$$

where $R \equiv |r|^2$ is the reflection probability of the domain-wall region. In arriving at Eq. (7), we have focused on the case of the charge pumped by a steady state of the domain wall moving with a constant velocity $v = \gamma H \delta_w/\alpha$ and $\dot{\Phi} = 0$. This regime is established when the strength of the external magnetic field is below the so-called Walker breakdown field, i.e., $H < H_W$ [24]. Here, from the equation of motion for the magnetic angle in Eq. (5), this Walker breakdown field is, in turn, set by the Dzyaloshinskii-Moriya field as $H_W = \alpha H_D$. We note that, in general, $I_1 + I_2 \neq 0$, reflecting the fact that charge can be repopulated along the edges, adding a capacitive energy cost to the free energy of our magnetoelectric system [27]. However, focusing, for clarity, on systems which are mirror (about the xz plane) symmetric results in $I_1 + I_2 = 0$, as explained next.

First, we note that a simultaneous mirror (about the xz plane) and time-reversal transformation leaves the magnetic configuration and external fields invariant while interchanging k_1 with k_2 (and k_3 with k_4). Consequently, for the aforementioned mirror-symmetric case, we have $k_1 = k_2$ and $k_3 = k_4$. Additionally, we note that the two domains and corresponding chiral modes are related by time reversal, invoking which, we further get $k_1 = k_3$ and $k_2 = k_4$ [29]. Under these assumptions, substituting $k_1 = k_2 = k_3 = k_4 = k_F$ in Eq. (7), we arrive at the first main result of this Rapid Communication, $I_1 = -I_2 = I_p$, where the pumped current I_p is given by Eq. (1). This pumped current can also be understood in terms of charge pushed by a piston, having a reflection coefficient R, moving with a velocity v in a strictly one-dimensional wire [referred to here as the "1D piston" and sketched in Fig. 2(b)]. Taking, for simplicity, a Galilean invariant 1D piston with quadratic energy dispersion, i.e., $E(k) = \hbar^2k^2/2m$ (with m being the effective mass of fermionic particles at low temperature), the particle current dragged by the piston can be calculated by going into the frame of reference where the piston is static. In this frame, the wave vectors get boosted as $k \to k + \delta k$, with $\delta k = mv/\hbar$. Consequently, the energy difference between the left and the right movers, i.e., $\Delta E = 2(\partial E/\partial k)\delta k$, appears as an effective bias voltage given by $eV_{\text{eff}} = \Delta E = 2\hbar k_F v$. Given the reflectivity of the piston is R, the Landauer-Büttiker charge current in the frame of reference of the piston is then given by $I_p = (R-1)e^2V_{\text{eff}}/h = (R-1)evk_F/\pi$. Finally, transforming this current back in the wire frame, the pumped current becomes $I = Revk_F/\pi$, establishing the equivalence mentioned above. Having found the charge pumped by a moving domain wall, we get $\mathcal{L}_{qx} = \gamma e \delta_w R/\alpha M_s dW$ using Eqs. (1) and (5). Invoking Onsager reciprocity [25,28], we then get $\mathcal{L}_{xq}$, which, when combined with Eq. (5), gives the other main result, i.e., an electrical bias-induced effective field given by Eq. (2).

Microscopically, the reflection coefficient governing the efficiency of this effective field is determined by the intermixing of the chiral modes at the domain-wall region.

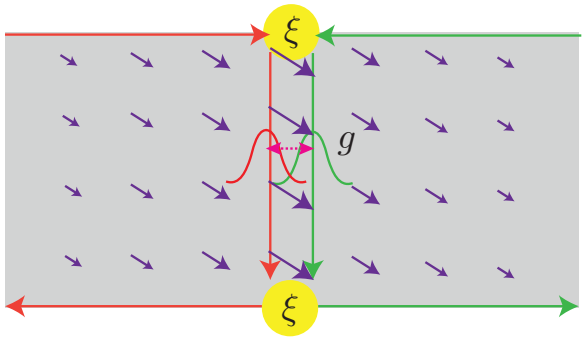

FIG. 3. Depiction of the intermixing process in the domain-wall region: The red and the green channels, i.e., the modes emanated from the left and right contacts of Fig. 1, can intermix upon reaching the domain-wall region. This intermixing is facilitated by two processes: (i) Sharp turns in the conduction path at either end of the domain wall, represented by circular scatterers with transmission probability ξ. (ii) During propagation along the domain wall, tunneling can occur between the modes due to the finite width of each mode (as depicted by the overlap of two Gaussians), which is parametrized by the tunneling conductance per unit length g.

Recently, such an intermixing process has been discussed in the context of edge state mixing in the quantum Hall state of graphene [30]. There are two sources of this intermixing process, which are illustrated schematically in Fig. 3. First, the potentially abrupt change in the direction of propagation at the beginning and the end of the domain wall (as indicated by the circular scatterer) can result in a distribution of charges between the chiral modes. Due to conservation of current, this distribution can be parametrized by a single parameter ξ, denoting the transmission probability of each such scatterer. Second, during the propagation of modes along the domain wall, proximity-induced finite tunneling (as parametrized by a tunneling conductance per unit length g) can also result in the equilibration process. The reflection coefficient is then given by [30]

$$R = \frac{1 + (1-2\xi)^2 e^{-W/\lambda}}{2}, \tag{8}$$

where $\lambda \equiv e^2/2gh$ is defined as the equilibration length for intermode scattering during propagation along the domain wall. When the full equilibration between the chiral modes occurs by scattering at the start and end of the domain wall, i.e., for $\xi = 1/2$, the reflection coefficient becomes independent of the sample width, just as the spin-Hall angle, and takes a value of $R = 1/2$. On the other hand, in the regime when the intermixing at the sharp turns can be neglected, i.e., $\xi = 0$, the width of the sample as compared to equilibration length becomes an additional important parameter governing R. For $W \gg \lambda$, the reflection coefficient again approaches the value of $R = 1/2$. Consequently, θ_V for the proposed mechanism can quite generally be expected to approach a universal value of 2.

Quantitative estimates. We focus on magnetic TI structures with material parameters based on a Cr-doped $(Bi,Sb)_2Te_3$ system [17]. In this case, $A \sim k_B T_c/a \sim 4 \times 10^{-8}$ erg/cm, where $T_c = 30$ K is the Curie temperature and $a \sim 1$ nm is the typical distance between two Cr atoms, while $K = 5 \times 10^4$ erg/cm^3 and $M_s = 10$ emu/cm^3. For estimating the largest possible pumped current ($I_{\max}$), while still maintaining our low energy description based on the QAH insulator phase, we have $k_F \sim \Delta/\hbar v_F$. Here, v_F parametrizes the linear dispersion of the form $E(k) = \hbar v_F k$ for the chiral modes, and 2Δ is the gap opened in the surface state dispersion due to exchange coupling to magnetic order. Using this, we get $I_{\max} \sim eRv\Delta/hv_F$. The Fermi velocity for the chiral modes is the most uncertain parameter here, estimating which from the typical surface state Fermi velocity $v_F = 10^5$ m/s [31], using $\Delta \sim 0.1$ eV [32] and $v = \gamma H\sqrt{A}/\alpha\sqrt{K} \sim 100$ m/s (for applied $H = 10$ Oe and $\alpha \sim 0.01$), we get $I_{\max} \sim 4$ nA. Next, the effective magnetic field for an applied bias of $eV = \Delta = 0.1$ eV and a typical nanowire geometry with $W = 100$ nm and $t = 5$ nm is estimated to be $H_V = 2\pi R\hbar I_q/e\lambda_F M_s t W \sim 1$ Oe. Consequently, the expected order of current-induced domain-wall velocity is given by $v \sim 10$ m/s. We note that the proposed phenomenon is well within the reach of experimental observation in present day magnetically doped topological insulators (where the QAH phase has been observed up to $\sim$2 K [33]), while alternative large gap systems, such as Ref. [34], could provide possible candidates for room temperature applications. It should be emphasized that the main results of our phenomenological theory (expressed in terms of reflection coefficient) are valid for any QAH insulator.

Acknowledgement. This work was supported by FAME (an SRC STARnet center sponsored by MARCO and DARPA). Discussions with So Takei, Yabin Fan, and Kang Wang are gratefully acknowledged.

[1] J. E. Moore, Nature (London) **464**, 194 (2010); M. Z. Hasan and C. L. Kane, Rev. Mod. Phys. **82**, 3045 (2010); X.-L. Qi and S.-C. Zhang, *ibid.* **83**, 1057 (2011).

[2] O. Pankratov, Phys. Lett. A **121**, 360 (1987); C.-X. Liu, X.-L. Qi, X. Dai, Z. Fang, and S.-C. Zhang, Phys. Rev. Lett. **101**, 146802 (2008); X. Z. Yu, Y. Onose, N. Kanazawa, J. H. Park, J. H. Han, Y. Matsui, N. Nagaosa, and Y. Tokura, Nature (London) **465**, 901 (2010).

[3] X.-L. Qi, T. L. Hughes, and S.-C. Zhang, Phys. Rev. B **78**, 195424 (2008); A. M. Essin, J. E. Moore, and D. Vanderbilt, Phys. Rev. Lett. **102**, 146805 (2009).

[4] F. Wilczek, Phys. Rev. Lett. **58**, 1799 (1987).

[5] X.-L. Qi, R. Li, J. Zang, and S.-C. Zhang, Science **323**, 1184 (2009).

[6] K. Nomura and N. Nagaosa, Phys. Rev. B **82**, 161401 (2010).

[7] I. Garate and M. Franz, Phys. Rev. Lett. **104**, 146802 (2010).

[8] Y. Tserkovnyak and D. Loss, Phys. Rev. Lett. **108**, 187201 (2012).

[9] Y. Ferreiros, F. J. Buijnsters, and M. I. Katsnelson, Phys. Rev. B **92**, 085416 (2015); Y. Ferreiros and A. Cortijo, *ibid.* **89**, 024413 (2014).

[10] J.-J. Zhu, D.-X. Yao, S.-C. Zhang, and K. Chang, Phys. Rev. Lett. **106**, 097201 (2011); Y. Tserkovnyak, D. A. Pesin, and D. Loss, Phys. Rev. B **91**, 041121 (2015).

[11] G. Tatara, H. Kohno, and J. Shibata, Phys. Rep. **468**, 213 (2008).
[12] S. S. P. Parkin, M. Hayashi, and L. Thomas, Science **320**, 190 (2008).
[13] D. A. Allwood, Science **309**, 1688 (2005).
[14] E. O. Lachman, A. F. Young, A. Richardella, J. Cuppens, H. R. Naren, Y. Anahory, A. Y. Meltzer, A. Kandala, S. Kempinger, Y. Myasoedov, M. E. Huber, N. Samarth, and E. Zeldov, Sci. Adv. **1**, e1500740 (2015).
[15] M. Liu, W. Wang, A. R. Richardella, A. Kandala, J. Li, A. Yazdani, N. Samarth, and N. P. Ong, arXiv:1603.02311.
[16] S. Grauer, S. Schreyeck, M. Winnerlein, K. Brunner, C. Gould, and L. W. Molenkamp, Phys. Rev. B **92**, 201304 (2015).
[17] C.-Z. Chang, J. Zhang, X. Feng, J. Shen, Z. Zhang, M. Guo, K. Li, Y. Ou, P. Wei, L.-L. Wang, Z.-Q. Ji, Y. Feng, S. Ji, X. Chen, J. Jia, X. Dai, Z. Fang, S.-C. Zhang, K. He, Y. Wang, L. Lu, X.-C. Ma, and Q.-K. Xue, Science **340**, 167 (2013); X. Kou, S.-T. Guo, Y. Fan, L. Pan, M. Lang, Y. Jiang, Q. Shao, T. Nie, K. Murata, J. Tang, Y. Wang, L. He, T.-K. Lee, W.-L. Lee, and K. L. Wang, Phys. Rev. Lett. **113**, 137201 (2014).
[18] Y. Fan, P. Upadhyaya, X. Kou, M. Lang, S. Takei, Z. Wang, J. Tang, L. He, L.-T. Chang, M. Montazeri, G. Yu, W. Jiang, T. Nie, R. N. Schwartz, Y. Tserkovnyak, and K. L. Wang, Nat. Mater. **13**, 699 (2014).
[19] S. Emori, U. Bauer, S.-M. Ahn, E. Martinez, and G. S. D. Beach, Nat. Mater. **12**, 611 (2013); K.-S. Ryu, L. Thomas, S.-H. Yang, and S. Parkin, Nat. Nanotechnol. **8**, 527 (2013).
[20] Y. Tserkovnyak and S. A. Bender, Phys. Rev. B **90**, 014428 (2014).
[21] A. Hoffmann, IEEE Trans. Magn. **49**, 5172 (2013).
[22] I. E. Dzyaloshinskii, Sov. Phys. JETP **5**, 1259 (1957); T. Moriya, Phys. Rev. **120**, 91 (1960).
[23] A. A. Thiele, Phys. Rev. Lett. **30**, 230 (1973); O. A. Tretiakov, D. Clarke, G.-W. Chern, Y. B. Bazaliy, and O. Tchernyshyov, *ibid.* **100**, 127204 (2008).
[24] N. L. Schryer and L. R. Walker, J. Appl. Phys. **45**, 5406 (1974).
[25] L. Landau and E. Lifshitz, *Statistical Physics, Part 1* (Pergamon, Oxford, UK, 1980), Vol. 5.
[26] L. Pitaevskii and E. Lifshitz, Statistical Physics, Part 2 (Butterworth-Heinemann, Oxford, UK, 1980), Vol. 9; A. Thiaville, S. Rohart, E. Jue, V. Cros, and A. Fert, Europhys. Lett. **100**, 57002 (2012).
[27] M. Büttiker, H. Thomas, and A. Prêtre, Z. Phys. B **94**, 133 (1994); P. W. Brouwer, Phys. Rev. B **58**, R10135(R) (1998).
[28] G. E. W. Bauer, S. Bretzel, A. Brataas, and Y. Tserkovnyak, Phys. Rev. B **81**, 024427 (2010).
[29] Assuming the time-reversal symmetry breaking by an external magnetic field is not significant to affect the dispersion of chiral modes.
[30] S. Takei, A. Yacoby, B. I. Halperin, and Y. Tserkovnyak, Phys. Rev. Lett. **116**, 216801 (2016).
[31] H. Zhang, C.-X. Liu, X.-L. Qi, X. Dai, Z. Fang, and S.-C. Zhang, Nat. Phys. **5**, 438 (2009).
[32] X. F. Kou, W. J. Jiang, M. R. Lang, F. X. Xiu, L. He, Y. Wang, Y. Wang, X. X. Yu, A. V. Fedorov, P. Zhang, and K. L. Wang, J. Appl. Phys. **112**, 063912 (2012).
[33] M. Mogi, R. Yoshimi, A. Tsukazaki, K. Yasuda, Y. Kozuka, K. S. Takahashi, M. Kawasaki, and Y. Tokura, Appl. Phys. Lett. **107**, 182401 (2015).
[34] S.-C. Wu, G. Shan, and B. Yan, Phys. Rev. Lett. **113**, 256401 (2014).